

Mechanical Properties and Cross-Linking Density of Short Sisal Fiber Reinforced Silicone Composites

Rajasekaran Karthikeyan,^{a,b,*} Jimi Tjong,^a Sanjay K. Nayak,^b and Mohini M. Sain^a

In the low cost application of vacuum casting in rapid prototyping, a mould cavity with high modulus is necessary for producing plastics parts in small quantity. In this work, a silicone matrix was reinforced with natural fibers to improve the modulus of composites to mould and to reduce the cost of silicone materials. Sisal fiber with different compositions was reinforced with silicone in a compression moulding process. Mechanical properties were studied. An increase in tensile strength, tear strength, and better hardness was observed in sisal fiber composites. The silane-treated fiber improved the adhesion between fiber and matrix and enhanced the mechanical properties of the composites. The swelling method was adopted to determine the cross-linking density of composites through the Flory-Rehner equation. The flexibility of silicone composites decreased for higher fiber loading and there was an increase in cross-linking of the fiber network to improve modulus of the composites. A morphological study was conducted using X-ray tomography and scanning electron microscopy (SEM) to predict the defects, orientation, debonding, fractography, and interfacial adhesion of fiber/matrix composites.

Keywords: Natural Fibers; Silicone composites; Compression process; Mechanical Property; Morphological study; Optical microscopy; Cross-linking density

Contact information: a: Faculty of Forestry, University of Toronto, 33 Willcocks Street, Toronto, ON M5S 3B3, Canada; b: Advanced Research School for Technology & Product Simulation (ARSTPS), Central Institute of Plastics Engineering & Technology (CIPET), Guindy, Chennai -600 032, India;

* Corresponding author: rajasekaran.karthikeyan@mail.utoronto.ca

INTRODUCTION

Polymer composites are commonly used in engineering applications, where fibers are embedded in a polymer to increase their mechanical properties (Thielemans and Wool 2004). Silicone rubber is an insulating material that is used to develop silicone moulds and produce thermosetting parts in small volumes at reduced cost (Windecker 1977; Weber and Kamal 1992). The use of silicone moulds in rapid prototyping (RP) technology could produce a newly designed product in quick time and develop small volumes of parts for functional testing. Rapid tooling (RT) is an extension of RP, where a silicone mould is developed from RP parts to produce small volumes of products (Rosochowski and Matuszak 2000; Gebhardt 2007). Moreover, no attempt has been made to reduce the cost of silicone mould in RT and to offer attractive features such as tear strength, high modulus, hardness, *etc.*

Natural fibers are being used in polymer composites to increase the strength and make eco-friendly to the environment (Arumugam *et al.* 1989). Cellulose fibers are abundantly available at a lower cost and are combined with rubber to enhance the mechanical properties of rubber composites (Boustany and Arnold 1976). Varghese *et al.*

have reported the increase of mechanical and viscoelastic properties of short sisal fiber reinforced natural rubber composites and studied the effect of chemical treatment on fiber loading (Varghese *et al.* 1994; John *et al.* 2008). However, limited research attention has been devoted to silicone composites to evaluate the use of sisal fiber as reinforcement.

The physical structure of natural fiber consists of cellulose, hemicelluloses, lignin, and waxes, which together establish a poor interface and generally hydrophilic nature, which decreases the strength of composites. Therefore, chemical treatment is necessary to enhance the compatibility of fiber /matrix adhesion and hydrophobic nature in fiber (Li *et al.* 2007). In studies of the effect of alkali treatment on sisal fiber, 4% NaOH treatment resulted in maximum tensile strength (Geethamma *et al.* 1995; Jacob *et al.* 2004). The silane treatments were implemented to reduce the proportion of hydroxyl groups and establish a covalent bond with the cell wall of sisal fiber (Herrera-Franco and Aguilar-Vega 1997). The formation of hydrocarbon chain during silane treatment may resist the swelling of fiber and establish a covalent bonding of cross-link network between fiber and matrix (Varghese *et al.* 1994; Herrera-Franco and Aguilar-Vega 1997).

Cross-linking is an entanglement of the polymer chain network and is evaluated by the degree of swelling in solvent through the Flory-Rehner equation (Barlkani and Hepburn 1992). The modulus of elastomeric materials is related to the degree of cross-linking, where a lower degree of cross-linking results in higher degree of swelling and tends to have low modulus and flexible material (Keshavaraj *et al.* 1994; Da Costa *et al.* 2001). Many researchers have studied the swelling behavior of short fiber reinforced elastomeric composites. George and Thomas (1999) studied the effect of cross-linking density on swelling and mechanical properties of styrene-butadiene rubber (Kumar *et al.* 1995). Varghese *et al.* (1994) investigated the adhesion between sisal fiber and rubber using equilibrium swelling method. There is little information available on the effect of cross-linking density for different fiber loading in silicone composites.

There has been a lack of research on the low cost manufacturing of silicone composite moulds for RT application. There are a few studies documenting fiber reinforced natural rubber composites, but there has been no significant work on the effect of fiber loading in silicone composites. Furthermore, the cross-linking density of silicone composites has not been predicted using the Flory-Rehner equation and the swelling method. The defects, fiber dimension, microstructure, and interfacial adhesion between the fiber/matrix composite have not been analyzed using non-destructive methods.

In this study, sisal fiber was treated with 3-amino propyl triethoxysilane and reinforced with silicone sealant in a compression moulding process, and its mechanical and morphological characteristics were studied. The properties of tensile, hardness, and tear strength were compared for both treated and untreated sisal fiber composites. The swelling test was performed to predict cross-linking density of composites using the Flory-Rehner equation. The microstructure was examined using X-Ray tomography and SEM analysis, and the fiber/matrix interaction and defects in silane-treated fiber composites were studied.

EXPERIMENTAL

Materials

The commercial resin silicone-methyl tri (ethyl methyl ketoxime) silane was used as the viscous fluid and obtained from Dow Corning from DAP, Inc. (Scarborough,

Canada). The viscous resin is a single component moisture-cured polymer and has low intermolecular forces. The physical properties of silicone resin were as follows: density, 0.982 gm/cc; specific gravity, 1.03; and service temperature, 0 °C to 200 °C. The sisal fiber was obtained from M/s Vibrant Nature (Chennai, India). The sisal fiber had a density of 1.34 gm/cm³ and strength of 650 to 700 M Pa (Ramesh *et al.* 2013).

Fiber treatment

All the sisal fibers were pretreated with 1% NaOH solution for the partial removal of lignin, wax content, and undesirable material. The treatment was carried out at room temperature for 2 h, and the fiber was washed with distilled water until neutral pH was attained. The whole process was carried out two times to remove the wax content and to generate roughness on the surface of the fiber. The fibers were then chopped to an average length of 3 mm and sieved to maintain uniform size. The short fibers were further treated with silane to reduce the proportion of cellulose hydroxyl groups at the fiber surface; the possible chemical reaction is shown in Fig. 1. The presences of alkoxy groups in silane are hydrolyzed to form silanol. The hydroxyl group present in the fiber reacts with silanol to form stable covalent bonds to cell wall of the fiber. The silane (3-amino propyl triethoxy silane) (2% by weight) was dissolved in distilled water for 5 min, and the sisal fibers were immersed in this solution for 2 h at room temperature for silane hydrolysis. Therefore it is anticipated that the reaction of the silane with the water took place rapidly, giving rise to colloidal matter, which might not be sufficiently active to react with the cellulosic surfaces according to Fig. 1. Fibers were washed with distilled water for removal of acid until they reached a pH of 4.5 to 5.5. Then the fiber was dried in air for 2 h and subsequently oven-dried for 12 h at 75 °C, and stored in polythene bags to prevent moisture (Xue *et al.* 2007).

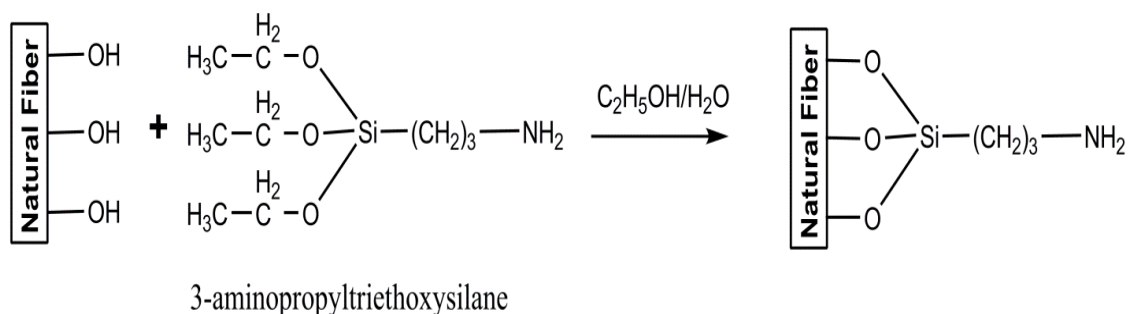


Fig. 1. Schemes of interaction of silane with natural fiber

Compounding process and specimen preparation

The fiber was chopped to a length of 3 mm for short fiber and 10 mm for long fiber with diameter less than 0.4 mm. Chopped fibers were mixed with silicone uniformly in a Brabender, Plasti-Corder[®] Lab-Station (Duisburg, Germany). The mixer was driven at a rotor speed of 50 rpm with maximum torque 150 Nm for 10 min to achieve uniform mixing at room temperature. The sisal/silicone composition in wt.% was prepared for both treated and untreated sisal fiber. The composite specimens were developed for 5%, 10%, 15%, and 20%, of sisal fiber reinforced silicone composite. The tensile specimen was developed in compression moulding at room temperature, as per standard test method of tensile test ASTM D412-15a (2015). The tear specimen was developed in

compression moulding as per standard test method of tear test ASTM D624-00 (2012). The thermosetting silicone composites were moisture cured over air for 96 h to form cross-linked molecular bonds in all composites.

Mechanical Characterization

Tensile test

The tensile test was performed using an Instron 3367 tensile testing machine (Norwood, MA, USA) equipped with load cell 30000N and accuracy of 10 μ m. The testing process was carried out at a crosshead speed of 50 mm/min and a gauge length of 33 mm, and the average value of tensile and modulus was recorded for 10 samples of treated and untreated sisal fiber silicone composites. The tear test was performed as per ISO 34-1 (2015) for 6 samples in the Instron tensile testing machine with a gauge length of 50 mm for both treated and untreated sisal fiber composites.

Hardness

The hardness was measured using a Shore A type durometer (Zwick, Ulm, Germany) and followed ASTM D2240-05 (2010). The depth of indentation on flat, cured specimens was measured for a given period of 10 s at 10 different locations on the composites. The average value of Shore A hardness number was tabulated.

Swelling test

The cross-link density of sisal fiber reinforced silicone composites was determined by a swelling test, performed in xylene solvent at room temperature. The specimen was cut to 20 mm \times 20 mm \times 3 mm and weighed before being immersed in the solvent. Composites were immersed in a jar containing xylene solvent for 72 h, and the swollen composites was weighed for calculating cross-link density (Da Costa *et al.* 2001; Marzocca and Mansilla 2007). From the experimental data, the molar volume of solvent and volume fraction of swollen composites were calculated for cross-link density in moles/g using the Flory-Rehner equation (Barlkani and Hepburn 1992; Gan *et al.* 2008).

Morphological Study

Scanning electron microscopy

Scanning electron microscopy (SEM) (S-3400 SEM, Hitachi Ltd., Ibaraki, Japan) was used to analyze fracture surfaces of the composites and to visualize the differences between treated and untreated natural fiber. The micropores, voids, microstructures, and interfacial interaction of fiber and matrix were investigated with the scanning electron microscope with a magnification factor (500 X) and an accelerating voltage of 5.00 kV.

The fracture surfaces of tensile composites were mounted on stubs and gold-sputtered to establish effective conductivity for examination. The images were processed using software to measure the cross-section, fibers, and voids.

X-ray tomography

The short fiber orientations in the composite were visualized, and dimension of the fiber were measured using USB Digital Microscope at 10 \times to 150 \times magnification. The composite defects and fiber deformations on the surface were examined using an optical microscope (Model # 44302-A, Celestron, Torrance, USA). The internal structures of fiber arrangement in the matrix were examined using non-destructive technique by X-ray computed tomography (CT) (Phoenix nanotom, GE, AZ). The

scanning was performed using nano-focus tube at 8.56 μm voxel resolution of 23.35 \times magnification, and it investigated voids, uncured matrix, and improper adhesion from composites.

Fourier Transform Infrared (FTIR) Spectroscopy

The FTIR analysis was performed on both treated and untreated fiber and studied the constituents of sisal fiber. The spectra of the fibers were recorded using Agilent Cary 630 FTIR spectrometer (US).

RESULTS AND DISCUSSION

Tensile Strength of Composites

The tensile strength of the sisal fiber composites is understood to depend on interfacial interaction of fiber/matrix, orientation, and fiber length. The tensile strength for various compositions of untreated and treated fibers is graphically represented in Fig. 2. The incorporation of short fibers in silicone material decreased the strength of the composites. This is due to weak interfacial bonding between short fibers and resin due to waxes on the surface of fibers. A remarkable improvement in tensile strength was observed for silane-treated short fiber, which established a better interfacial bonding between the fiber surface and matrix. The increase in fiber interaction was attributed to an increase in surface roughness and pores on the treated fibers (Fig.10 (b)). This resulting from lignin removal by the treatment with NaOH (Sun *et al.* 2011) and then the fiber was treated with silane. The evidence of lignin removal was also discussed in the FTIR section.

Figure 2 shows that silane treatment resulted in a considerable increase in tensile strength of 10%, 15%, and 20% sisal fiber composites. The incorporation of 20% treated sisal fiber in silicone matrix allowed an enhancement of 20% tensile strength of the composites compare to virgin silicone. This improvement in strength may be due to removal of impurities on fiber surfaces and mechanical interlocking of rough fibers with the matrix.

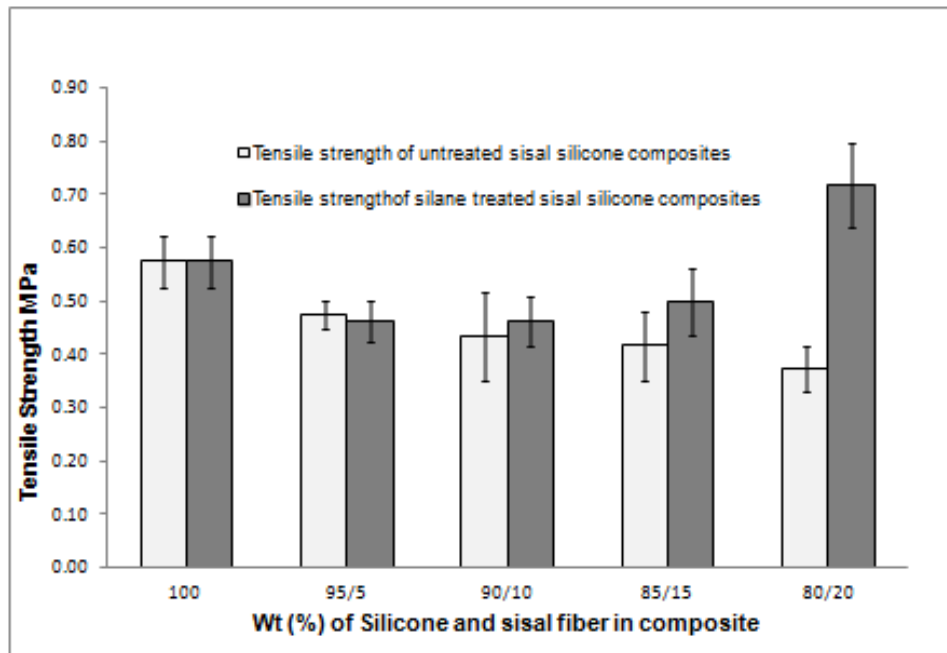


Fig. 2. Tensile strength of untreated and treated sisal fiber reinforced silicone composites

The silane treatment reduces the amount of exposed hydroxyl groups of cellulose at the fiber-matrix interface. The hydrolyzable alkoxy groups react with moisture to form silanol. Further, the silanol react with the hydroxyl group of the fiber to form covalent bonds to the cell wall on the fiber surface to give a better interface between fiber and the matrix.

Tensile Modulus

The modulus of elasticity of a composite depends on the volume fraction of fiber and the distribution of fiber in the matrix. The tensile modulus of treated and untreated fibers reinforced with silicone composites is presented in Fig. 3. The incorporation of fibers in the matrix increased the modulus of the composites for both treated and untreated fibers. This result indicated that modulus depended on the fiber volume fraction and did not depend as much on length of the fiber. The tensile modulus of 20% fiber composites was 2.44 MPa, which was higher than virgin silicone (0.48 MPa) because of reinforcement effect of short fibers in composites. A similar effect was observed in treated fiber reinforced composites, and the modulus value for 20% fiber composition was 2.98 MPa, which was 22% higher than untreated fiber composites. Composite strength depended on the mean aspect ratio and mean fiber length, but composite modulus depended on the fiber volume fraction and fiber distribution.

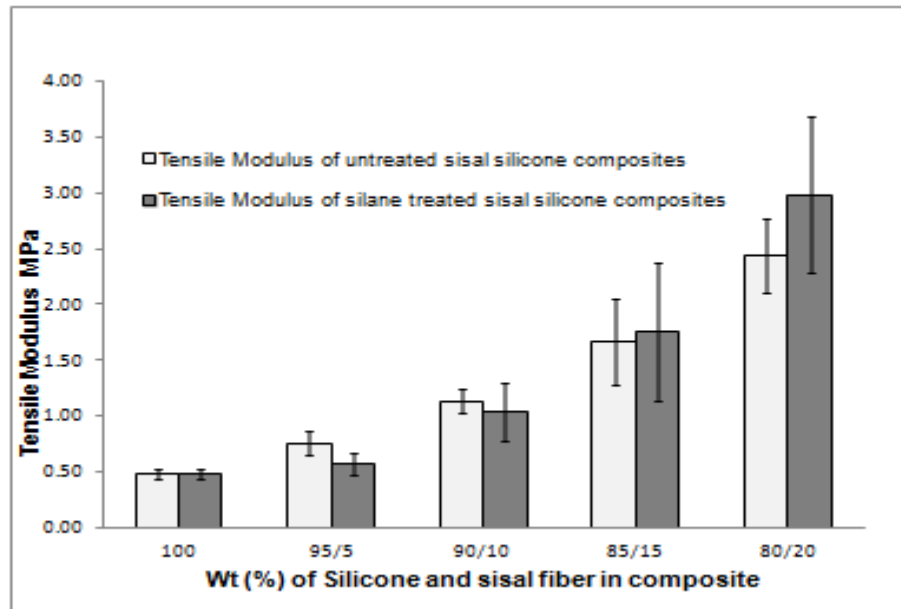


Fig. 3. Tensile modulus of untreated and treated sisal fiber reinforced silicone composites

Hardness of Composites

The hardness of short fiber reinforced elastomers depends on fiber concentration and fiber distribution. However, increased hardness results in better interaction between matrix and short fibers. Figure 4 shows the Shore A hardness of silane-treated and untreated sisal fiber reinforced silicone composites. The hardness of the silicone fiber composites increased for fiber composition of 5%, 10%, 15%, and 20%. The incorporation of fiber enhanced the composites, making them harder and stiffer. The increases in fiber volume fraction improved the modulus and hardness due to enhancement of the cross link density. Figure 4 shows that the Shore A hardness of silane-treated silicone composites was improved for each fiber composition compared with untreated silicone composites. The hardness of treated sisal fiber composites for 20% composition was 10% higher than the untreated fiber composites; this result was attributed to better adhesion between fiber-silicone matrix and enhanced network structures within the cross-linked system.

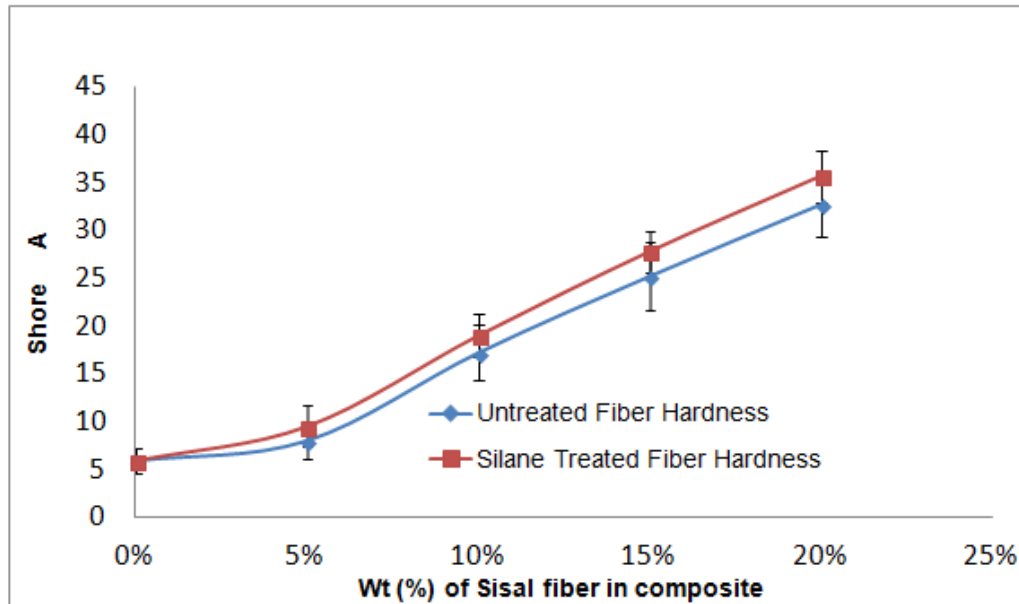


Fig. 4. Hardness of untreated and treated sisal fiber reinforced silicone composites

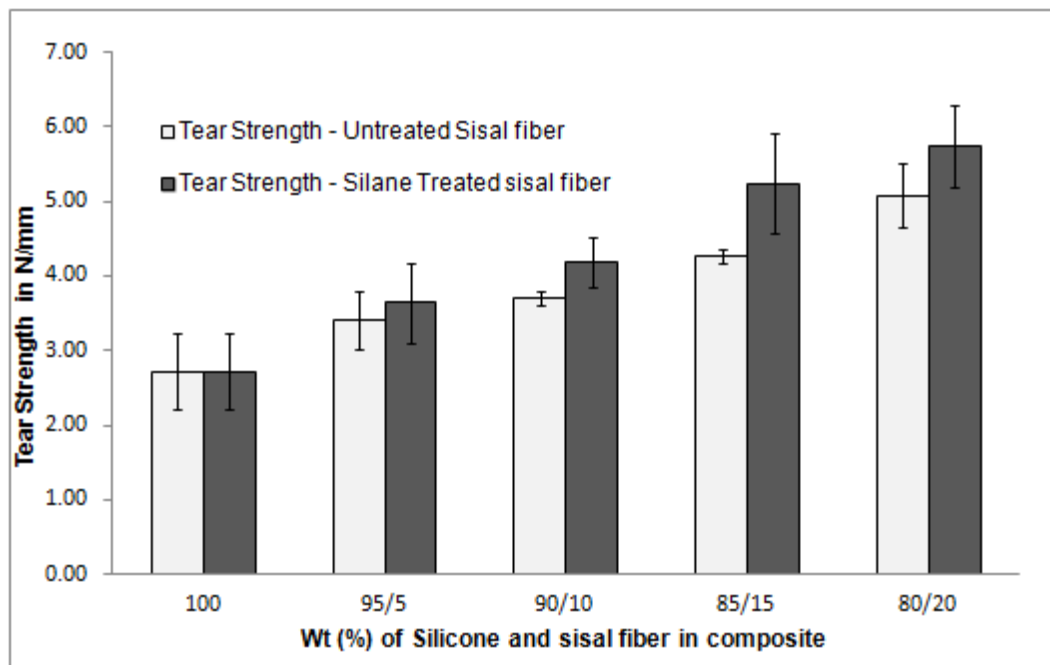


Fig. 5. Tear strength of silane-treated and untreated sisal reinforced composites

Tear Strength

Tear resistance describes the material strength of elastomers under the action of static force and kinetic forces on tearing. The right angle tear strength of the silicone material was 2.72 N/mm, as measured by a tensile testing machine. Figure 5 shows the tear strength with various percentages of fiber composition for both treated and untreated sisal fibers. The incorporation of short fibers in silicone material increased the tear strength. The tear strength of the composite for 20% fiber loading was 5.08 N/mm, which was increased by 80% compared with virgin silicone. This result is due to the short fibers

being aligned along the direction of loading, which was perpendicular to direction of tear propagation. Therefore, the short fibers transferred stress around and prevented crack growth. The concentration of short fibers increases tear strength by obstructing the tear path. Figure 5 shows that treated fiber enhanced the tear strength. The tear strength for 20% composites was remarkably increased by 13% compared with untreated composites. Also, there was a 23% increase in tear strength for composition of 15% compared with treated and untreated sisal fiber silicone composites. The increase in concentration and fiber-matrix adhesion resulted in an improved stiffness and modulus of short fiber composites. Also the load acting on the matrix was transferred to fiber and reduced the crack growth rate.

Cross-Linking Density

The cross-linking density of polymer composite is a major factor influencing the mechanical behavior of fiber filled and unfilled elastomers. The degree of cross-linking in elastomeric material was determined by a swelling method. The Flory-Rehner equation was used to calculate the network cross-linking density, where molecular weight M_c between the cross-link network is inversely proportional to cross-link density. Figure 6(a) shows the cross-linking density for various percentages of fiber loading composites. The cross-linking density for 20% of fiber loading was 5.19×10^7 moles/m³, which may resist swelling due to the presence of fillers and reduce the penetration of xylene into silicone composites. There were fewer moles of crosslinking in a low volume fraction of fiber composites, which increased the gap of neighboring molecules to enable flexibility in the swollen specimen. The increase of fiber loading might decrease the uptake of solvent in cured composites and resist swelling which may attribute to better interfacial adhesion. Therefore, the increase in cross-link density might increase material stiffness, modulus, and hardness of silicone composites.

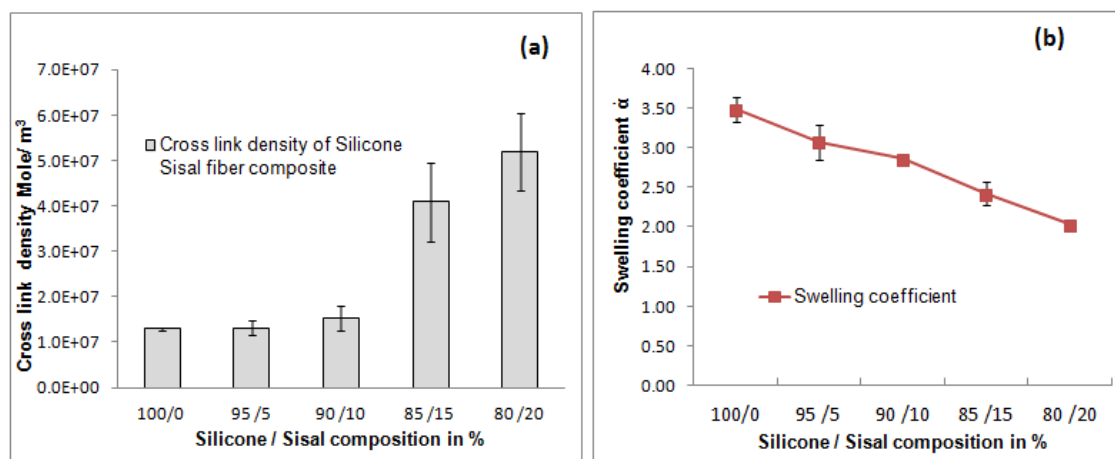


Fig. 6. (a) Cross-linking density, (b) Swelling coefficient of silicone composites

The swelling coefficient is a measure of swelling resistance of silicone composites (Fig. 6(b)). There was a gradual decrease in swelling coefficient seen in Fig. 6(b) for an increase in fiber loading. This indicates resistance in uptake of solvent by composites due to rigid bonding established between fiber and matrix. There was variation in swelling coefficient at specific fiber loading due to the effect of fiber orientation in composites. There was a maximum swelling capacity in the composites,

which were extended in a direction normal to the fiber orientation. This is due to the fact that penetration of solvent in the matrix was prevented by fibers, where the fibers are arranged in perpendicular direction to the sample surface. Higher values of swelling coefficient having a low number of moles in unit volume led to weak Si-O bonding and enhanced flexibility in the low volume fraction of fiber loading.

Effect of Fiber Length on Mechanical Property

Certain parameters affect the performance of fiber reinforced silicone composite such as fiber concentration, fiber aspect ratio, degree of fiber dispersion, fiber/rubber matrix adhesion, and voids. The interaction between matrix and fiber enables resistance to elongation. Thus, the tensile strength of short fiber and long fiber composites were compared for 5%, 10%, and 15% of fiber loading (Fig. 7).

As shown in Fig. 7(a), the incorporation of short fiber in silicone composites remarkably decreased its strength, thereby causing a low interfacial bonding between fiber and matrix. The composites prepared with a fiber length greater than 10 mm showed improved mechanical properties due to the better mechanical interlocking and fiber matrix interaction.

The fiber adhesion with matrix was improved by roughening the contact surface area of the fiber. Therefore, the tensile strength was remarkably increased for various compositions of long fiber composites (Fig. 7(a)). Also, the increase in strength was due to extended stress transfer on fiber length and fiber/matrix interfacial adhesion.

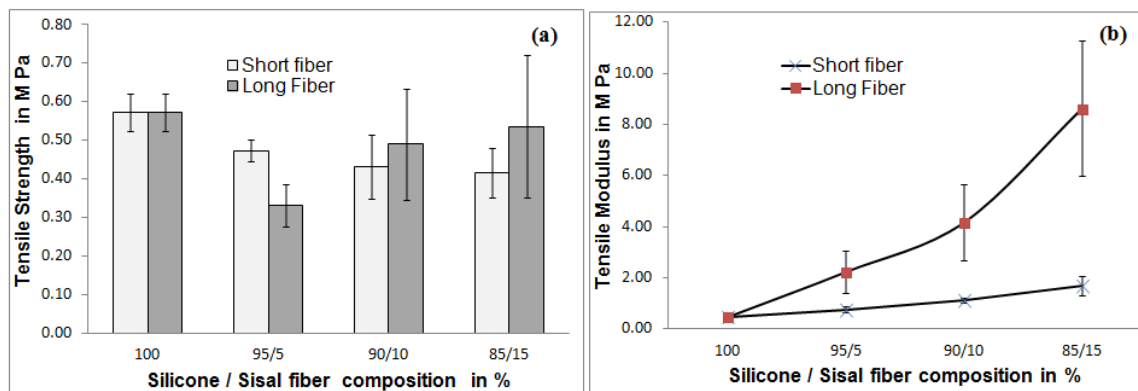


Fig. 7. (a) Tensile strength for long fiber and short fiber; (b) tensile modulus for long fiber and short

An increase in fiber concentration can remarkably improve the modulus of elasticity of composites, whereas the volume fraction of long and short fiber of the same composition influences the modulus of composites. Thus, there was a remarkable increase in modulus for 5%, 10%, and 15% fiber loading of elongated fiber composites (Fig. 7(b)). There was an increase in modulus for 15% of long fiber composites due to entanglement of fiber and reinforcement effect of fibers. The long fiber transferred an increased amount of stress on a high fiber volume fraction, which enhanced the modulus.

Morphological Analysis

Fiber orientation

The microstructure of composites such as fiber distribution, fiber-fiber interaction, fiber orientation, fiber/matrix interaction, voids, and air bubbles was studied using X-ray tomography and optical microscopy (Fig. 8). It was observed that sisal fibers were randomly oriented in the composites (Fig. 8(a)). Further voids and improper interfacial adhesion were observed on sliced sections of composites through non-destructive techniques. This will contribute to failure of composites and reduce the tensile strength and modulus. Figure 8(b) shows that surface defects such as entrapped air bubbles, fiber-fiber interaction, and micro-fibrils viewed under an optical microscope. These defects may initiate failure that results in composite fracture.

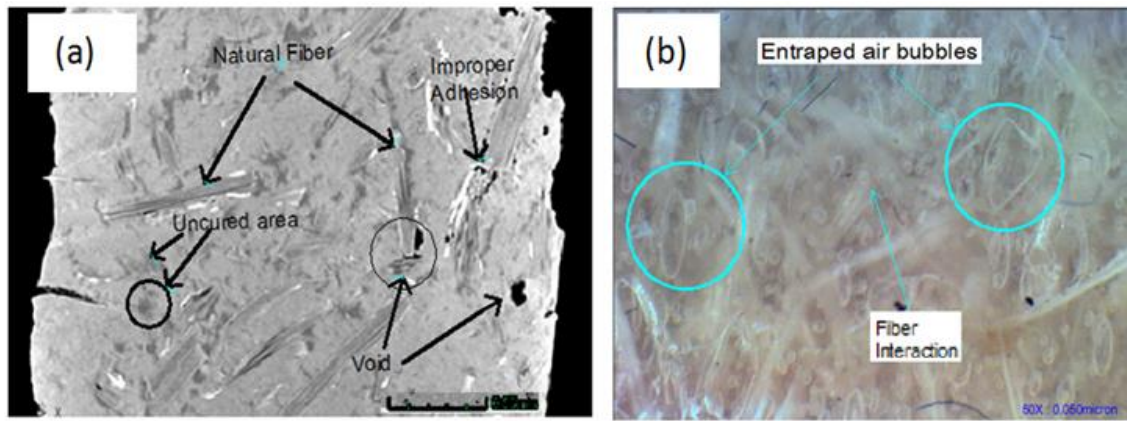


Fig. 8. (a) X-ray tomography image of fibers composites; (b) defects in sisal fiber reinforced silicone composites

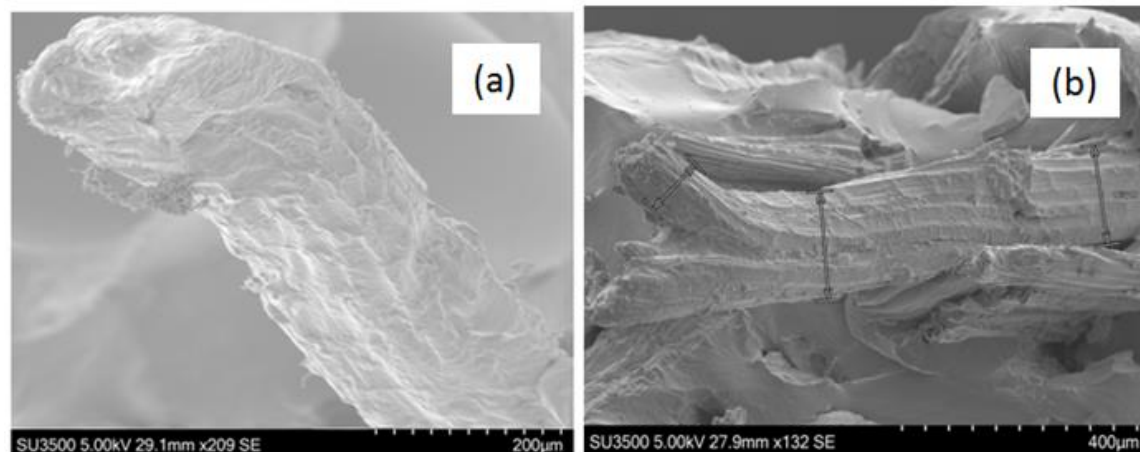


Fig. 9. (a) Untreated fiber, (b) silane-treated fiber

SEM Analysis

Fiber surface

Surface impurities and physical irregularities on the fiber surface were examined by SEM (Fig. 9). Node-like materials representing lignin appeared on the surface of fibers (Fig. 9(a)). Untreated sisal fibers were smooth on their surfaces due to the presence of wax and lignin, which hinder interfacial interaction with the matrix. Figure 9(b) shows

the surface of treated fiber, which contained rough irregularities. This was attributed to better mechanical interlocking between fiber and matrix due to the removal of wax and node-like materials. While physical changes in the fiber and surface texture were inspected by SEM, adsorption of silane on the surface of fiber might significantly improve the adhesion (Belgacem and Gandini 2005).

Fractography

Fractographic techniques are used to find the cause of failure in fiber-reinforced composites (Fig. 10). The distribution of sisal fiber in the silicone matrix was random, and fiber pull-out holes confirmed the poor adhesion with silicone. This debonding was due to tensile forces at the fiber ends exceeding the tolerance of silicone, causing the elastomer to shear at the interface and pull out. There are microspores on the fiber surface that contribute to interfacial failure. Micro-pores result from the removal of lignin and hemicelluloses during fiber treatment (Shi *et al.* 2011). Figure 10(c) shows the poor adhesion of fiber matrix interaction and pull-out holes in composites, resulting in bonding failure. Figure 10(d) shows good adhesion with fiber tearing and fracture of fibers. This results in increased tensile strength. Also, poor adhesion at the fiber-matrix interface, air holes, and debonding were observed, which may initiate cracks to fail the composite during tensile modes.

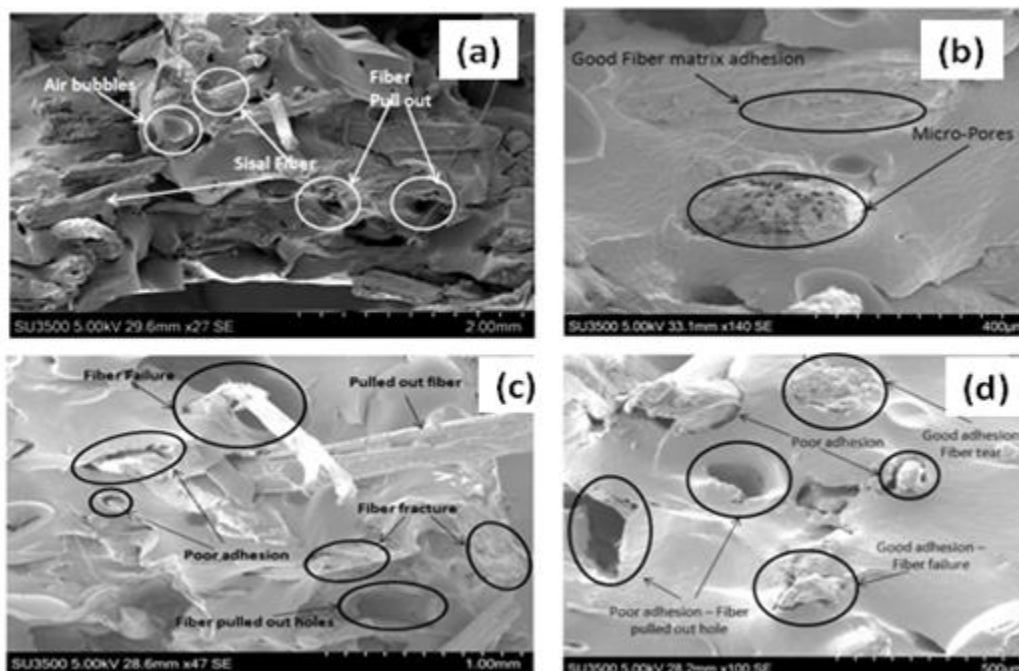


Fig. 10. SEM micrographs (a) after tensile fracture; (b) fiber micro-pores and good adhesion; (c) fiber fracture and poor adhesion; and (d) pullout holes and fiber tear

Fourier Transform Infrared Spectroscopy (FTIR) Analysis

The functional groups of the sisal fiber were analyzed using FTIR spectroscopy, and the spectra of untreated and silane-treated fiber are displayed in Fig. 1. It was noted that a peak appeared in the band spectra 3150 to 3350 cm^{-1} , which reveals the hydrogen bonded (O-H) in the lignin and cellulosic structure of the sisal fiber. The intensity of the peaks in the spectral range 1010 to 1170 cm^{-1} reveal the primary and secondary hydroxyl

groups corresponding to C-O-C stretching. The peaks that are near 1720 cm^{-1} correspond to -C=O stretching, revealing the presence of aliphatic carboxylic acid. The intense peak at 1045 cm^{-1} denotes the C-O band of the primary hydroxyl group in the unmodified fiber.

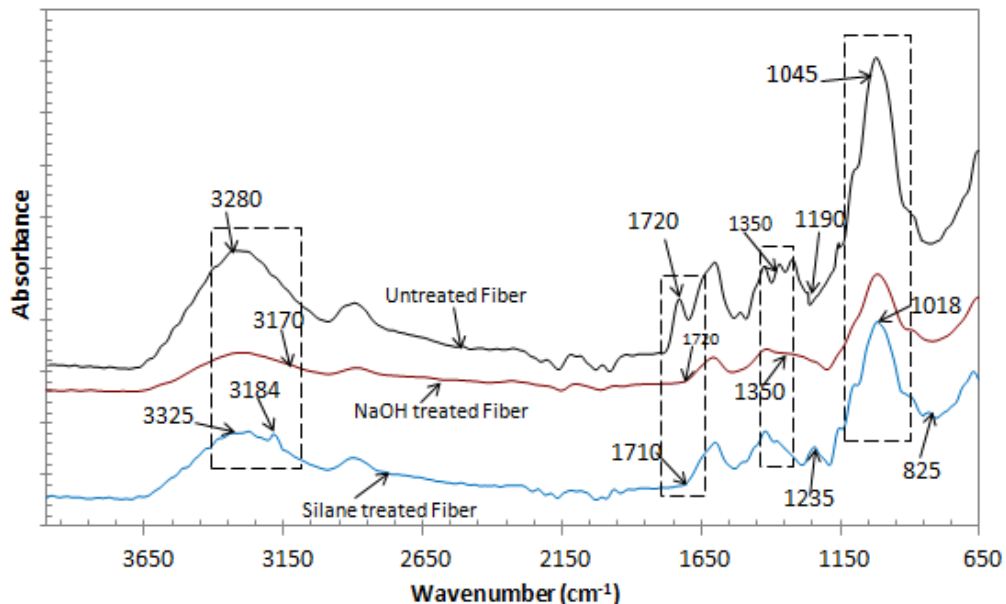


Fig. 11. FTIR spectra for untreated and treated sisal fibers

The presence of Si-O-C was noticed in the cellulose of silane-treated sisal fiber, having a stretching vibration in the broad spectra of 1000 to 1190 cm^{-1} . The intensity of the peak near 1018 cm^{-1} indicates the Si-O-C band, and an increase in C-O stretching of cellulose was evident after silane treatment. The FTIR spectra show a small peak at 825 cm^{-1} in modified fiber compared to unmodified fiber, which can be attributed to a strong absorption of Si-O. However, the amino group of NH_2 stretching band was introduced to the fiber at 3184 cm^{-1} with 3-amino propyl triethoxysilane treatment. It was observed that the peak at 1720 cm^{-1} corresponds to the presence of lignin in the untreated fiber. This peak disappeared after the successive treatment with NaOH, indicating the partial removal of lignin. The carbonyl group of stretching vibration was observed in the bands of 1710 cm^{-1} and 1650 cm^{-1} . The intensity of the absorption band at 1720 cm^{-1} was reduced due to subsequent treatment of natural fiber with NaOH to confirm the partial dissolve of lignin. The major composition of lignocelluloses fibers having cellulose, hemicelluloses, lignin, and also minor constitutes of pectin, waxes and water soluble components were reduced, which was observed by the spectra of silane-treated fiber (Derkacheva and Sukhov 2008; Fan *et al.* 2012).

The vibration peak at 1350 cm^{-1} corresponds to OH in untreated fiber disappeared after chemical treatment resulting in removal of hemicellulose. The band 1235 cm^{-1} in untreated fiber shows the presences of both lignin and pectin attributed to C-O ring of lignin, which was removed after surface treatment of fiber (Paluvai *et al.* 2015).

The peak at 3100 to 3300 cm^{-1} reveals that stretching vibration of hydrogen bonding (OH) of untreated fiber was decreased in the spectra of silane-treated fiber. This confirms the removal of hemicelluloses and decrease of the carboxyl group in the fiber (Ganan *et al.* 2002). Also, the vibration peak at 3184 cm^{-1} corresponds to the stretching of

the C-H aliphatic group of all natural fibers which was decreased after treatment due to the removal of hemicelluloses. It was observed from untreated fiber that the peak at 1045 cm^{-1} was reduced after treatment with NaOH. This indicates a reduction in lignin content and observed roughness on the surface of the fiber in SEM.

CONCLUSIONS

1. The incorporation of silane-treated sisal fiber in silicone improved the tensile strength of composites with 10%, 15%, and 20% fiber loading. There was an increase in tensile strength by 25% for 20% of fiber loading compared with silicone material. The series of treatments increased the roughness on the contact surface of the fiber and provided a better mechanical interlocking between fiber and matrix.
2. The tensile modulus for various fibers loading was increased for both treated and untreated fiber composites, where treated composite for 20% fiber loading was higher than untreated composites by 22%.
3. The tensile modulus of treated sisal silicone composites of 15% and 20% was increased compared with virgin silicone and untreated sisal silicone composites. The modulus of the composites was increased due to the reinforcement effect of fiber with resin.
4. The incorporation of short fibers in silicone increased hardness and tear strength of composites for both treated and untreated fiber. Treated fiber composites were superior to untreated composites, and a maximum increase in tear strength for 15% of composite by 23% was observed.
5. The cross-link density was predicted using the swelling method, and the hardness of fiber composites was higher for 15% and 20% of fiber loading. The entanglement of fiber in the composites resists the uptake of solvent and limits molecular motions of the siloxane chain segments.
6. The microstructure of composites was analyzed using SEM and X-ray tomography, and the following defects were observed: debonding, poor adhesion, micro-air bubbles, fiber fracture, and micropores on fiber surfaces.

ACKNOWLEDGEMENTS

The authors greatly acknowledge the Centre for Biocomposite and Biomaterial Processing (CBBP), University of Toronto, and the Department of Chemicals and Petrochemicals (DCPC), Govt. of India, for supporting funds in the CoE Project, in the Green Transportation Network (GREET).

REFERENCES CITED

- Arumugam, N. K. T. S., Selvy, K. T., Rao, K. V., and Rajalingam, P. (1989). "Coconut fiber reinforced rubber composites," *J. Appl. Polym. Sci.* 37(9), 2645-2659. DOI: 10.1002/app.1989.070370916

- ASTM D412-15a (2015). "Standard test methods for vulcanized rubber and thermoplastic elastomers - Tension," ASTM International, West Conshohocken, USA.
- ASTM D624-00 (2012). "Standard test method for tear strength of conventional vulcanized rubber and thermoplastic elastomers," ASTM International, West Conshohocken, USA.
- ASTM D2240-05 (2010). "Standard test method for rubber property—Durometer hardness," ASTM International, West Conshohocken, USA.
- Barlkani, M., and Hepburn, C. (1992). "Determination of crosslink density by swelling in the castable polyurethane elastomer based on 1/4-cyclohexane diisocyanate and para-phenylene diisocyanate," *Iranian J. Polym. Sci. Technol.* 1(1), 1-5. DOI: 10.1002/app.31643
- Belgacem, M. N., and Gandini, A. (2005). "The surface modification of cellulose fibres for use as reinforcing elements in composite materials," *Compos. Interfaces* 12(1-2), 41-75. DOI: 10.1163/1568554053542188
- Boustany, K., and Arnold, R. L. (1976). "Short fibers rubber composites: The comparative properties of treated and discontinuous cellulose fibers," *J. Elastomers Plast.* 8(2), 160-176. DOI: 10.1177/009524437600800202
- Da Costa, H. M., Nunes, R. C. R., Visconte, L. L. Y., and Furtado, C. R. G. (2001). "Physical properties and swelling of natural rubber compounds containing rice husk ash," *Raw Mater. App.* 54(5), 242-249. DOI: 10.1002/app.10125
- Derkacheva, O., and Sukhov, D. (2008). "Investigation of lignin by FTIR spectroscopy," *Macromol. Symp.* 265(1), 61-68. Wiley-VCH Verlag., DOI: 10.1002/masy.200850507
- Fan, M., Dai, D., and Huang, B. (2012). "Fourier transform infrared spectroscopy for natural fibers," *Fourier Transform – Materials Analysis. InTech.* DOI: 10.5772/35482
- Gan, T. F., Shentu, B. Q., and Weng, Z. X. (2008). "Modification of CO₂ and its effect on the heat-resistance of silicone rubber," *Chin. J. Polym. Sci.* 26(04), 489-494. DOI: 10.1142/s0256767908003163
- Ganan, P., and Mondragon, I. (2002). "Surface modification of fique fibers. Effect on their physico-mechanical properties," *Polym. Compos.* 23(3), 383-394. DOI: 10.1002/pc.10440
- Gebhardt, A. (2007). *Understanding Additive Manufacturing: Rapid Prototyping, Rapid Tooling, Rapid Manufacturing*, Carl Hanser, Munich, Germany. DOI: 10.3139/9783446431621
- Geethamma, V. G., Joseph, R., and Thomas, S. (1995). "Short coir fiber reinforced natural rubber composites: Effects of fiber length, orientation, and alkali treatment," *J. Appl. Polym. Sci.* 55(4), 583-594. DOI: 10.1002/app.1995.070550405
- George, S. C., and Thomas, S. (1999). "Effect of nature and extent of crosslinking on swelling and mechanical behavior of styrene-butadiene rubber membranes," *J. Membr. Sci.* 163(1), 1-17. DOI: 10.1016/s0376-7388(99)00098-8
- Herrera-Franco, P. J., and Aguilar-Vega, M. D. J. (1997). "Effect of fiber treatment on the mechanical properties of LDPE-henequen cellulosic fiber composites," *J. Appl. Polym. Sci.* 65(1), 197-207. DOI: 10.1002/(sici)1097-4628(19970705)65

- ISO 34-1 (2015). "Rubber, vulcanized or thermoplastic - Determination of tear strength - Part 1: Trouser, angle and crescent test pieces," International Organization for Standardization, Geneva, Switzerland.
- Jacob, M., Thomas, S., and Varughese, K. T. (2004). "Mechanical properties of sisal/oil palm hybrid fiber reinforced natural rubber composites," *Compos. Sci. Technol.* 64(7), 955-965. DOI: 10.1016/s0266-3538(03)00261-6.
- John, M. J., Varughese, K. T., and Thomas, S. (2008). "Green composites from natural fibers and natural rubber effect of fiber ratio on mechanical and swelling characteristics," *J. Nat. Fibers* 5(1), 47-60. DOI: 10.1080/15440470801901480
- Keshavaraj, R., and Tock, R. W. (1994). "Modeling of changes in crosses linking for structural silicone sealants subjected to moisture and sunlight," *Polym. Plast. Technol. Eng.* 33(5), 537-550. DOI: 10.1080/03602559408010746
- Kumar, R. P., Amma, M. L., and Thomas, S. (1995). "Short sisal fiber reinforced styrene-butadiene rubber composites," *J. Appl. Polym. Sci.* 58(3), 597-612. DOI: 10.1002/app.1995.070580315
- Li, X., Tabil, L. G., and Panigrahi, S. (2007). "Chemical treatments of natural fiber for use in natural fiber-reinforced composites: A review," *J. Polym. Environ.* 15(1), 25-33. DOI: 10.1007/s10924-006-0042-3
- Marzocca, A. J., and Mansilla, M. A. (2007), "Analysis of network structure formed in styrene-butadiene rubber cured with sulfur/TBBS system," *J. Appl. Polym. Sci.* 103(2), 1105-1112. DOI: 10.1002/app.25264
- Paluvai, N. R., Mohanty, S., and Nayak, S. K. (2015). "Studies on thermal degradation and flame retardant behavior of the sisal fiber reinforced unsaturated polyester toughened epoxy nanocomposites," *J. Appl. Polym. Sci.* 132(24), DOI: 10.1002/app.42068
- Ramesh, M., Palanikumar, K., and Reddy, K. H. (2013). "Comparative evaluation on properties of hybrid glass fiber-sisal/jute reinforced epoxy composites," *Procedia Eng.* 51, 745-750. DOI:10.1016/j.proeng.2013.01.106
- Rosochowski, A., and Matuszak, A. (2000). "Rapid tooling: The state of the art," *J. Mater. Process. Technol.* 106(1), 191-198. DOI: 10.1016/s0924-0136(00)00613-0
- Sun, R., Song, X., Sun, R., and Jiang, J. (2010). "Effect of lignin content on enzymatic hydrolysis of furfural residues," *Bioresources* 6(1), 317-328. DOI: 1279-5735-1-PB
- Shi, J., Shi, S. Q., Barnes, H. M., Horstemeyer, M. F., and Wang, G. (2011). "Kenaf bast fibers—Part II: Inorganic nanoparticle impregnation for polymer composites," *Int. J. Polym. Sci.* 2011, 1-7. DOI: 10.1155/2011/736474
- Thielemans, W., and Wool, R. P. (2004). "Butyrate kraft lignin as compatibilizing agent for natural fiber reinforced thermoset composites," *Compos. Part A Appl. Sci. Manuf.* 35(3), 327-338. DOI: 10.1016/j.compositesa.2003.09.011
- Varghese, S., Kuriakose, B., Thomas, S., and Koshy, A. T. (1994). "Mechanical and viscoelastic properties of short fiber reinforced natural rubber composites: Effects of interfacial adhesion, fiber loading, and orientation," *J. Adhes. Sci. Technol.* 8(3), 235-248. DOI: 10.1163/156856194x01086
- Weber, M. E., and Kamal, M. R. (1992). "Mechanical and microscopic investigation of whisker-reinforced silicone rubber," *Polym. Compos.* 13(2), 133-145. DOI: 10.1002/pc.750130208

Windecker, L. J. (1977). "Silicone rubber mold," U.S. Patent No. 4,051,296. DOI:
10.1787/888932889535

Article submitted: June 20, 2016; Peer review completed: August 7, 2016; Revised
version received: September 5, 2016; Accepted: October 2, 2016; Published: November
14, 2016.

DOI: 10.15376/biores.12.1.211-227.